PORT AND OCEAN ENGINEERING UNDER ARCTIC CONDITIONS
TECHNICAL UNIVERSITY OF NORWAY

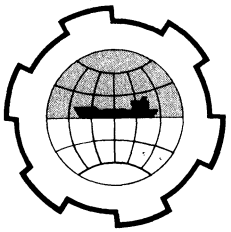

LONG-PERIOD WAVES IN AN ICELANDIC FJORD

R. Dorrestein, Netherlands
P. Bruun, Norway
A. Juliusson, Iceland

This paper describes the results of research on long-period waves carried out in Eyjafjördur, an Icelandic fjord located in North Iceland on the Arctic Ocean (Fig. 1).

RESEARCH PROGRAM, INSTRUMENTATION

Eyjafjördur (Fig. 1) is approx. 60 km long and has a 30 km long, 10 km wide outer section and a 30 km long, 2-5 km wide funnel-shaped inner section. Depths generally range from 40 to 100 meters. The fjord is subject to heavy gales from the northern quadrant. The main tidal constituent is the semidiurnal M_2 tide. Mean tidal range is approx. 0,9 meter in the entire fjord.

A tide recorder installed at Olafsfjördur at the entrance to the fjord revealed the existence of waves of approx. 20 min period in the 5 km long side fjord, almost directly connected to the ocean.

To investigate the behavior of long period waves in the fjord a research project was undertaken in 1964, based on a grant from the Office of Naval Research, Dept. of the Navy, to the University of Florida, Dept. of Coastal Engineering, where Prof. J. Purpura administered the contract. Considerable practical assistance of any kind was offered by the Icelandic Department of Ports and Lighthouses. Analyses were carried out in Holland by Dr. Dorrestein assisted by Mr. A.C.M. van Ette of the Hydraulic Laboratory at Delft.

Eight long-period wave recorders comprising ordinary modified Leupold & Stevens type tide recorders werè installed in Eyjafjördur and at Grimsey (island located approx. 40 km north of the mainland).

The location of the gauge stations Olafsfjördur, Hrisey, Hauganes, Hjalteyri, Dagverdaeyri, Akureyri North (Oddeyri) and Akureyri South (Hafnarbryggja) is shown in Fig. 1. As the western part of the fjord is more densely populated and includes a number of piers making the installation and supervision problem easier, all the stations were established on that side of the fjord. The Leupold & Stevens tide recorders had electric clocks. Ratio of height scale was 1:10 and paper speed 6 inches per hour.

At the sites the gauges were installed in a case on top of a 10 inch steel well so the float and counter-weight could move freely with the rise and fall of water inside the well. The well itself was securely fastened to a pier or quay at the station (Fig. 2).

The interior of the well was of conical shape at the lower end on which a heavy bottomlid made of ironplates rested. The bottomlid was of similar conical shape, but with a rubber gasket to make a tight seal with the conical section of the well. A chain led from the bottomlid to the top of the well, on which there was an opening through which the bottomlid could be lifted for inspection and cleaning.

The orifice of the well was in the bottomlid. Its diameter was 1/4 inch only, in order to filter out sea and swell activity. It had to be inspected and cleaned from time to time to prevent clogging.

This arrangement of the bottomlid proved inadequate in some places, where the well was very much exposed to strong wind wave activity causing the bottomlid to be lifted up from its seat whereby the recorded trace was disturbed.

This was avoided by placing extra lead weights on top of the lid but in extreme cases, where even that was not enough, a pipe was welded to the outside of the well and a chain led through. The chain was fastened to an eye bolt on the down side of the bottomlid and at the upper end a rigging-screw was attached to tighten the

chain so the bottomlid would make a watertight seal. This proved satisfactory in all cases and did not cause too much inconvenience when cleaning the orifice.

This research set-up worked satisfactorily. Checking of timing was made with very accurate stop-watches operated by all the attendants. Due to small frequency irregularities in the power supply between some stations checking of timing was always necessary. Unfortunately, these frequency variations were so large at Grimsey that the Grimsey records could not be used for analyses.

As mentioned above gales from N - NE with wind forces of 9 Beaufort (40 mph) or more are relatively frequent during the winter months. As soon as such gales approached the Eyjafjördur area, gauges were started and run for at least 72 hours continuously. During the runs they were inspected several times per day by the attendants who made timecheck marks on the records which were used to correlate records from the various stations.

THEORY AND ANALYSES

a. General

A brief account on theory and analyses of records undertaken by the first author, Dr. Dorrestein, is given in the next sections. The most conspicuous feature of all water level records is the semidiurnal tide. The shorter period long waves, even those which are amplified in the fjord by resonance, represent only a small fraction of the total variance of the water levels. In the theory, it is assumed that all long-wave activity in the fjord is of oceanic origin so that no energy is transferred from the atmosphere to long waves within the fjord proper, and the fjord responds as a passive system on an oceanic input signal. If moreover, non-linear effects in the fjord caused by turbulence friction of the currents would be negligible, the fjord would act as a linear passive system so that, after spectral analysis, the coherences of water levels between pairs of stations should be close to unity and the amplitude ratios and phase differences for any pair of stations should be the same functions of frequency for all records. It was assumed that the oceanic "input signal" and the water level "signals" in the fjord can be described as gaussian random signals for the period range below 6 hours. No indications could be found that this assumption would be incorrect. It was thought essential to extract from the available data the maximum of information. That is, since a linear description was

attempted, we aimed at a maximum resolution in the frequency domain. The most appropriate method then is straightforward Fourier analysis of sets of strictly simultaneous segments of water level records, together with the calculation of cross-spectral parameters.

The use of this method of analysis implies that no information was extracted from the records concerning possible instationarities, trends, or sequences of events within the duration of the records. Such information, though, was considered to be irrelevant here because the purpose of the analysis was to study the response of the fjord to waves coming from the ocean, and not so much to examine the origin and behaviour of these waves outside the fjord.

The general geometry of the fjord was shown by Fig. 1. For the theory we define $x(\geq 0)$ = longitudinal coordinate, with $x = 0$ at the closed head of the fjord, $b(x)$ = width of water surface and $d(x)$ = average depth across the fjord. The seaward boundary of the fjord, rather arbitrarily defined as a line running roughly W - E at 66°11' North, is then situated at $x = 60$ km. The width $b(x)$ and the mean depth $d(x)$, as approximated from the sea chart, have been plotted as functions of x in Figs. 3 and 4.

b. Theory.

The simplified, linearized theory of long gravity waves in channels (or narrow fjords or bays) with slowly varying cross section, either without or with some assumption of friction, with analytical solutions of the differential equations in special cases, can be found in several text books and articles; see e.g. (3, 4, 5, 6, 9, 14).

We shall use the following notation here in addition to x, b and d introduced in the previous section.

$A(x)$ = area of cross-section = $b(x) \cdot d(x)$
$h(x,t)$ = height of water surface above zero position
$q(x,t)$ = volume transport of water
$v(x,t)$ = velocity q/A
g = acceleration of gravity

If friction is neglected, and if we consider a harmonic wave motion given by

$$\left.\begin{aligned} h(x,t) &= H(x)\ \exp\ (i\omega t) \\ q(x,t) &= Q(x)\ \exp\ (i\omega t) \end{aligned}\right\} \text{(real part)} \qquad \text{(b1)}$$

with angular frequency ω, the differential equation for the amplitude $H(x)$ is

$$\frac{d^2H}{dx^2} + \frac{1}{A}\frac{dA}{dx} \cdot \frac{dH}{dx} + \frac{\omega^2}{gd} H = 0, \qquad \text{(b2)}$$

and Q can be found from

$$Q = i\,\frac{gbd}{\omega} \cdot \frac{dH}{dx} \qquad \text{(b3)}$$

It should be kept in mind that these equations can be expected to hold only 1≦ <u>inside</u> the fjord (not close to the entrance area adjacent to the sea) and 2≦ if the local wave length $2\Pi\,\omega^{-1}\,(gd)^{1/2}$ sufficiently exceeds the local width b of the fjord; if the minimum ratio would be 2, the minimum wave period for Eyjafjördur main fjord would be about 15 minutes.

To simplify eq. (b2) we introduce, following Schönfeld (14) a new dimensionless (real) independent variable s by:

$$s = \omega \int_0^x \frac{d\xi}{\sqrt{gd(\xi)}} \qquad \text{(b4)}$$

Then (b2) can be transformed into

$$\frac{d^2H}{ds^2} + \frac{1}{b\sqrt{d}}\,\frac{d}{ds}\,(b\sqrt{d}) \cdot \frac{dH}{ds} + H = 0 \qquad \text{(b5)}$$

and (b3) becomes

$$Q = ib\sqrt{gd} \cdot \frac{dH}{ds} \qquad \text{(b6)}$$

In considering (b5) and (b6) it has to be remembered, however, that b and d must still be considered as functions of x, not of s.

For certain simple assumptions for b(x) and d(x) analytical solutions of eqs.(b2) and (b5) can be found. One class of such solutions will be used here. We consider a "model fjord" for which (compare Fig. 4):

$$b(x) = \text{const. } x^m, \text{ m is a constant} \geq 0,$$
$$d(x) = \text{const. } x^n, \text{ n is a constant} \geq 0 \text{ and } < 2 \qquad \text{(b7)}$$

With (b7), (b4) becomes

$s/\omega = \text{const. } x^{1-n/2}$, (b5) turns into

$$\frac{d^2H}{ds^2} + \frac{1-2\alpha}{s} \cdot \frac{dH}{ds} + H = 0, \qquad \text{(b8)}$$

$$\text{with } \alpha = \frac{1-m-n}{2-n} \quad (\alpha \leq \tfrac{1}{2}),$$

and (b6) becomes:

$$Q = i \cdot \text{real const. } s^{1-2\alpha} \cdot \frac{dH}{ds} \qquad \text{(b9)}$$

The remarkable thing about eqs. (b8) and (b9) is that x and ω have disappeared, so that in the solutions x and ω appear exclusively combined in s, in such way that s/ω is a function of x only.

The solution of (b7) with the boundary condition Q = 0 at the closed head of the fjord s = 0 (see (b8)) can be shown to be (see e.g. (8)):

$$H = \text{const. } s^{\alpha} J_{-\alpha}(s) = \text{const.} \cdot K_{\alpha}(s), \qquad \text{(b10)}$$

where $J_{-\alpha}$ is the Bessel function of the first kind and order $(-\alpha)$ and where $K_{\alpha}(s)$ stands for the normalized function $s^{\alpha}J_{-\alpha}(s)$ such that $K_{\alpha}(0) = 1$.

Since $K_{\alpha}(s)$ is real for real s, the solution (b10), with (b4) represents a standing wave motion with nodes and antinodes, and in which the phase difference between any pair of stations is either 0° or 180°. For $\alpha < \frac{1}{2}$ the functions $K_{\alpha}(s)$ have damped

oscillatory character along the s-axis. For some values of α the solutions (b10) are well known functions:

$m = n = 0$ gives $\alpha = \frac{1}{2}$ and $K_\alpha = \cos s$,

$m + n = 1$ gives $\alpha = 0$ and $K_\alpha = J_o(s)$,

$m + \frac{3}{2}n = 2$ gives $\alpha = -\frac{1}{2}$ and $K_\alpha = \sin s/s$

The special cases (1º) $m = 1$, $n = 0$, $\alpha = 0$, (2º) $m = 0$, $n = 1$, $\alpha = 0$ and (3°)$m = 1$, $n = 1$, $\alpha = -1$ were dealt with briefly by Lamb (9) and were discussed more fully in (14, 4).

So far we neglected energy dissipation by fricton. Friction, however, was taken into account by several authors but in a strongly schematized way; this is permissible if the effect of friction on the resulting wave motions is relatively small. In most cases dealing with harmonic motion the friction term is linearized, i.e., the deceleration per unit mass is put proportional to the velocity v. We make the following generalized assumption on linearized friction in a harmonic motion: deceleration per unit mass=$p(x,\omega)$. v, in which the real, positive function $p(x,\omega)$ may, however, depend on the total wave motion in the fjord.
For the "model fjord" characterized by (b7) then the same solution (b10) turns out to be approximately valid, provided the real variable s according to (b4) is replaced by the complex variable:

$$s^* = \omega \int_o^x \frac{d\xi}{\sqrt{gd(\xi)}} - \tfrac{1}{2}i \int_o^x \frac{d\xi \cdot p(\xi,\omega)}{\sqrt{gd(\xi)}} = s(1-i\varepsilon) \qquad (b11)$$

and provided $p(x,\omega) << \omega$ so that also the real positive function $\varepsilon(x,\omega) << 1$. The function (b10), considered as function of the complex variable s^*, is analytical in a region including the positive real axis, and we have to consider now its behaviour along some line in the complex s^*-plane starting from the origin and running a little <u>below</u> the positive real axis with a small negative slope (see (8) for an illustration on this behaviour for the function J_o). Away from the zeros of $K_\alpha(s)$, $K_\alpha(s^*)$ will differ only relatively little from $K_\alpha(s)$.

The function $K_\alpha(s^*)$ according to (b10) with (b11), originated from the differential equation (b2) in x (with small friction term added). It is seen, however, that for a given station, $x = x_i$, in the "model Fjord" the complex ratio of the amplitudes there and at the head of the fjord (x=s=o), considered as function of the frequency ω, is given by $K_\alpha(s^*)$ with (b11) as well, i.e., with s being the real part of s^*, strictly proportional to ω. In section f it will be shown that this is, in fact, approximately true for Eyjafjördur.

The following table gives rough values of $2\pi(1488x60)^{-1}$. $s/\omega = s/k$, found by estimating the integral in (b4), using d(x) (Fig. 3), for different locations along the main fjord. (For the reason of the numerical factor, see section e).

Station	x(km)	s/k
Akureyri S	0	0
" N	2	0,010
Dagverdareyri	10½	0,040
Hjalteyri	20½	$0,073^5$
Hrisey	37½	0,124
(Mouth of Olafsfjördur)	(51-53½)	(0,164)
(Mouth)	(60)	(0,182)

c. Method of analysis

Let a record to be analysed be given by $h(\tau)$ for $\tau = t/T$ running from -1 to +1, where t is time and 2T is the total duration of the record of the order of 24 hours. We then put:

$$h(\tau) - \text{mean} \approx \sum_{k=1}^{k_{max}} a_k \cos k\pi\tau + \sum_{k=1}^{k_{max}} b_k \sin\pi k\tau \qquad (c1)$$

with the Fourier components a_k, b_k given by

$$a_k = \int_{-1}^{+1} h(\tau) \cos k\pi\tau \, d\tau, \quad b_k = \int_{-1}^{+1} h(\tau) \sin k\pi\tau \, d\tau \qquad (c2)$$

The contribution to the total variance of $h(\tau)$ that is given by the k th Fourier components is $\frac{1}{2}(a_k^2 + b_k^2) = \beta_k$. If this is divided by the elementary frequency step $(2T)^{-1}$, we obtain an

estimate of the spectral density W(f) at the frequency f = k/2T:

$$W_k = 2T\beta_k = T(a_k^2 + b_k^2) \qquad (c3)$$

This estimate has only two "degrees of freedom" (1, 2).

Actually, after having decided on the exact times of beginning, t_b, and end, t_e, of a set of record segments to be analysed, $t_e - t_b$ being an even number of minutes, the positions of beginning and end on each of the records were determined by linear interpolation from the preceding and the next time check as indicated on the records; then the ordinates on the chart records were sampled at equal time intervals very nearly equal to 2 minutes and for each of the records a corrected set of ordinates was computed for a time interval of exactly 2 minutes, assuming a linear relation between exact time and chart time over each range between two successive time checks. Then the Fourier components a_k and b_k were computed from (c2) after replacing the integral by a sum.

For the duration of the record segments to be analysed we choose, wherever possible, 24 h 48 min = 1488 minutes, closely approximating two cycles of the predominant M2-tide. With a standard sampling interval of 2 minutes, every set of ordinates then consists of 745 numbers and the Fourier components are computed up to $K_{max} = 372$, the "Nyquist frequency" (1, 2) being $(4 \text{ min})^{-1}$ = 4 1/6 mHz.

The choice of 1488 minutes was made in order to concentrate the energy of the large semidiurnal and diurnal tides as much as possible in the first two Fourier components, that is, to eliminate as much as possible the "contamination" introduced by these tides in the higher Fourier components.

It was found, however, that large low-frequency variations of the levels in the fjord associated mainly with large variations in air pressure (by inverse barometer effect) still caused large differences between the levels at the beginning and at the end of the segments and consequently gave rise to large "contaminations" in the higher frequencies.

This was overcome completely by "pre-tapering" the record segments, that is by multiplying the ordinates (after subtraction of their means) by a slowly varying tapering weighting function that falls off smoothly to zero at the beginning and at the end of the segment, prior to applying the Fourier analysis.

For this taper function we choose:

$$\cos^2 \frac{\pi}{2}\tau \equiv \tfrac{1}{2} + \tfrac{1}{2} \cos \pi\tau$$

In this case the modified Fourier components a'_k and b'_k can be simply expressed in the original ones:

$$\left.\begin{aligned} a'_k &= 1/4\ a_{k-1} + 1/2\ a_k + 1/4\ a_{k+1} \\ b'_k &= 1/4\ b_{k-1} + 1/2\ b_k + 1/4\ b_{k+1} \end{aligned}\right\} (k \geq 1) \qquad (c4)$$

The spectral estimates then in view of the gaussian assumption for $k \geq 5$, were computed as:

$$W_k = 8/3\ T(a'^2_k + b'^2_k) \quad (k \geq 5) \qquad (c5)$$

the factor 8/3 being the inverse value of the mean value of $\cos^4 \frac{\pi}{2}\tau$ between $\tau = -1$ and $\tau = +1$.

These estimates, again, have two "degrees of freedom", but there now is some positive correlation between W_k-values for neighbouring k s.

All of the analysed records were pre-tapered in the way just described.

In order to correlate pairs of records (numbered 1 and 2, say) the cross-spectral estimates were also computed, as given by (for pre-tapered records):

$$\left.\begin{aligned} C_{12,k} &= 8/3\ T(a_{1k}a_{2k} + b_{1k}b_{2k}) \text{ (cospectrum)} \\ Q_{12,k} &= 8/3\ T(a_{1k}b_{2k} - a_{2k}b_{1k}) \text{ (quadspectrum)} \end{aligned}\right\} (c6)$$

Averages of W_k, $C_{12,k}$ and $Q_{12,k}$ over 5 consecutive k-values (centered on multiples of 5) were computed and coherence estimates were derived from these averages (indicated by overbars) by

$$\gamma_k^2 = \frac{\overline{C_{12,k}}^2 + \overline{Q_{12,k}}^2}{\overline{W}_{1k} \cdot \overline{W}_{2k}} \qquad (c7)$$

These coherence estimates, however, are positively biased (see, e.g. (12)).

The sampling of the chart records, the correction for the timing deviations and the computations were supervised by Mr. A.C.M. van Ette of the Delft Hydraulics Laboratory. The computer used was a TR4 of the Technical University of Delft.

d. Records analysed

Simultaneous records from 3 to 7 stations were available from 5 periods of 4 to 6 days in the months Dec. 1966, Feb., March and Oct. 1967 and March 1968. The selection of sets of segments to be analysed was greatly determined by the occurring interruptions or failures in one of the records.

The main part of the conclusions was based on the analysis of 8 different simultaneous sets of segments from 3 to 5 stations along the fjord, all with duration 24 h 48 min, as given in the next table.

Nr.	Month	Day and local time	Stations * Hri	Hja	Dag	AkN	AkS	Tidal range (approx. cm)
1	Dec. 1966	9, 1500-10,1548			x	x	x	94
2	Feb. 1967	20, 1324-21,1412			x	x	x	62
3	"	21, 1412-22,1500	x	x	x	x	x	72
4	"	22, 1012-23,1100	x	x	x	x		88
5	Mar. 1967	14, 1612-15,1700	x	x	x	x	x	93
6	"	17, 0812-18,0900	x	x		x	x	77
7	"	18, 1400-19,1448	x	x			x	58
8	"	19, 1212-20,1300	x	x		x	x	53

* Hri = Hrisey
  Hja = Hjalteyri
  Dag = Dagverdareyri
  AkN = Akureyri (Oddeyri)
  AkS = Akureyri (Hafnarbryggja)

See fig. 1

Six sets of shorter durations from 1 to 4 stations, four of these sets including records of Olafsfjördur, were analysed as well.

e. Autospectra

Fig. 5 gives two examples of plots of spectral density estimate W_k vs. Fourier component number k, or frequency in mHz (=cycles per kilosecond). For the standard segment duration of 1488 min, one k-unit corresponds with $1488 \times 60 \text{ sec})^{-1}$ or 0,0112 nHz.

In spite of the large sampling variability per spectral estimate and the large variability from record to record, these Fourier spectra show some properties characteristic for each station and some general conclusions could be drawn. Nearly all spectra of AkS, Hja and Hri show pronounced peaks at or near k=12 or 0,135 mHz (period 124 min) and several spectra show peaks at or near k=27 or 0,30 mHz (period 55 min) and k=42 or 0,47 mHz (period 35 min). Here we clearly see the first, second and third mode of natural longitudinal oscillations in the main fjord.

If the theory of section b may be applied to the main fjord as a whole, the frequencies of the peaks of the autospectra, according to (b11) and (b10),should be directly proportional to the zero of the function $J_{-\alpha}(s)$, say s_1, s_2, s_3 etc. Since the ratios between the zeros, s_2/s_1, s_3/s_1 etc., are monotonous functions of the parameter α, a value for α can be derived from the ratios found between the resonant frequencies. Such an estimate is independent of the measured values of b(x) and d(x). From s_2/s_1 = 27/12 and from s_3/s_1= 42/12, we arrive at values -0,05 and -0,06, resp. for α. One of the combinations of values of m and n that lead to α = -0,05 is m = 0,68, n = 0,40, which values

represent a reasonable fit for the geometry of the fjord; see fig. 4.

The zeros s_1, s_2 and s_3 of the Bessel function $J_{-\alpha}(s)$ with $\alpha = -0,05$ are 2.49, 5.62 and 8.74, resp., so that the proportionality factor s/k for the whole fjord should be 2.49/12 = 5.62/27 = 8.74/42 = 0.208. This is some 15 percent higher than the last value given in the table at the end of section b for the mouth of the fjord, which is a confirmation of the well known fact (3, 13) that for a channel open to the sea with a width not quite negligibly small, the "effective length" for resonance exceeds the actual length by a certain amount.

The spectra of the stations along the main fjord show a general decrease with increasing frequency above 1 mHz, to a level of order 0,5 mm^2/mHz above 2 mHz, which is believed to be merely "instrumental noise" caused by the many sources of error coming in from the recording in Iceland to the print-out of the computer.

The four available spectra from the station Olafsfjördur, situated at the head of the small side fjord show common features that are, however, completely different from those of the main fjord stations. Peaks are found near 0,76, 1,65 and 2,43 mHz (periods 22, 10 and 7 minutes, respectively) and the best fit for α here is circa -0,3. The spectral density level does not decline with frequency above 1 mHz and is between 10 and 100 mm^2/mHz over most of the frequency range.

f. Amplitude ratios and phase differences

For each of the stations (i) on the main fjord and Akureyri S, the head of the fjord (A), plots were made of the amplitude ratio r calculated as $(W_{ik}/W_{Ak})^{\frac{1}{2}}$ (eq. (c5)), and of the phase difference ϕ, calculated as arc tg (Q_{iAk}/C_{iAk}) (eq. (c6)), both versus the Fourier component number k. Positive ϕ-values ($<180^o$) imply a phase lag for Akureyri S with respect to the first station.

The four examples of such plots given in figs. 6-9 illustrate that the theoretically expected behaviour (see section b) is approximated for frequencies up to about 0,5 mHz: 1º smooth curves can be drawn reasonably well through the points resembling plots of the modulus and phase of a function $K_\alpha(s^*)$ versus ω (eqs. (b10) and (b11)); 2º these curves are the same, or nearly so, for all segments of a given station and Akureyri S. There is, however, a certain amount of irregular scatter of the points, which varies for the different cases; this scatter, e.g., is seen to be relatively small in case 6 and higher in case 3 (which is the "worst" case). This shows that the non-coherent parts of the water levels in the fjord are not quite negligible.

The seven amplitude ratio curves for Hrisey and Akureyri S (examples figs. 6 and 7) show minima for k ca. 15 and ca. 39, associated with rather fast phase transitions over 180°. This shows that the fjord oscillations with these frequencies have nodes near Hrisey. The best estimate for the ratio between these frequencies from all cases, 2,54, leads to a value +0,24 as best fit for α for the inner part of the fjord landward of Hrisey. The fact that this value differs from the estimate of α for the whole fjord (section e) reminds us that the theory based on the assumption (b7) cannot be exactly valid. The value +0,24 for α is consistent with (e.g.) m=0,40, n=0,15, which are not unreasonable; see fig. 4.

The value +0,24 for α with the observed k-values also leads to s/k = 0,133 for Hrisey. This is a little higher than the value given in the table at the end of section b.

Since, by definition, the function $K_\alpha(s) = 0$ at the zeros s_1, s_2 etc., the minima of the amplitude ratio should, according to (b11), be approximated by

$$r_{min} \approx \varepsilon s_n \left|\frac{dK_\alpha}{ds}\right|_{s=s_n} , \qquad (f1)$$

where s_n is the n-th zero of $K_\alpha(s)$. Thus values for ε associated with these minima may be derived from estimated values for r_{min} and α. For the first minima we find r_{min}(average) = 0,14,

$\varepsilon = 0{,}10$, $\varepsilon s_1 = 0{,}20$; for the second minima r_{min}(average) = 0,17, $\varepsilon = 0{,}06$, $\varepsilon s_2 = 0{,}31$. The ε-values are, indeed, relatively small, as was presupposed for eq. (b11) to be valid. Owing to the scatter of the points in the r-plots, however, both estimates are certainly too high.

Finally, an independent estimate for α can be obtained from the ordinates of the secundary maxima of the r-plots, especially the first one, with ordinate (average) 0,68 at k about 27. The result in $\alpha = +0{,}30$, being only a little higher than the value +0,24 found earlier.

For Hjalteyri and Akureyri S the six amplitude ratio curves (examples figs. 8 and 9) show minima for k ablout 29 and the "best" ones show second minima for k about 70. Similar procedures as given above for Hrisey led to the following results.

The parameter α, as derived from the ratio between both frequencies, becomes +0,15; this is consistent with (e.g.) m=0,53, n= 0,20. The factor s/k then becomes 0,75.

For the dissipation parameters at the first minimum we find r_{min}(average) = 0,07, $\varepsilon = 0{,}05$, $\varepsilon s_1 = 0{,}11$; the latter value being smaller than both corresponding values found for Hrisey in accordance with the fact that εs, according to eq. (b11) should be an increasing function of x for given ω.

For Dagverdareyri and Akureyri S, the five r-plots show minima at k about 47 with minimum ordinates 0,13 to 0,21. Relevant parameters were estimated as for the other stations, but they appeared to be less accurate.

Even for Akureyri N and Akureyri S, separated by only 2 km, five similar plots could be made up to $k \approx 160$, which show their first minimum for k about 140 with minimum ordinates 0,3 to 0,5.

g. Closer analysis of the first resonance peak

In recent years much work has been done to obtain a better understanding of the response characteristics of harbours on

long waves incident upon an entrance gap; see (13, 11, 7, 10). The conditions at and near resonance are of special interest. Analytical and numerical, as well as hydraulic models were used. Few field measurements with subsequent analysis are known to have been made, however, to check the validity of such models. An attempt was made, therefore, to deduce the shape of the first resonance peak for Eyjafjördur as accurately as possible from the available field data.

This "resonance peak" is a function of frequency around the resonant frequency, which function will be defined here, either as (1º) the energy amplification factor at Akureyri S with respect to the wave motion "at sea", i.e., just outside the zone of disturbance caused by the presence of the fjord, or as (2º) the spectral density that would occur at Akureyri S if the spectral density "at sea" would be unity.

The difficulty, of course, is that no good water level records were available from outside the fjord taken simultaneously with records taken in the fjord. Therefore an indirect procedure had to be applied, necessarily involving a number of uncertainties. This procedure cannot be described in all details here. Essentially, it consists of two main steps.

The first main step is to estimate the ratios r_{Sk} of the amplitudes of the waves "at sea" and at Akureyri S for k = 10, 11, 12, 13 and 14 from 8 available autospectra of the latter station (see fig. 5) and from "intelligent guesses" at the simultaneous spectral densities "at sea". These guesses were made for each of the 8 cases individually, with the following assumptions: 1º complete coherence; 2º the amplitude ratio r_{Sk} for k = 7, 8, 9, 15, 16 and 17 (on both sides of the peak) is given by $|J_o(s)|$ with $s = (k/12)s_1$ (s_1 being the first zero 2.405); 3º the spectrum "at sea" in each case can be described by a power law as function of k (with negative exponent) over the range k = 7 to k = 17. The resulting estimates of r_{Sk}^{-1} for k = 10 to 14 incl. were averaged for the 8 cases and multiplied by $2/\sqrt{\pi}$ (correction factor for the sampling variability); fig. 10 shows the result.

The second main step is the "deconvolution" of the estimated r_{Sk}^{-2} values for k = 10 to 14 incl. with the spectral window function associated with the pre-tapered Fourier analysis, to find the real shape of the resonance peak. This spectral window function $P(|k-f|)$ is given in fig. 11 if $k >> 1$. It represents the fraction of the energy in the real spectrum associated with frequency f/2T that shows up in the k^{th} Fourier component. Actually, we assumed for the resonance peak the simple form

$$\frac{M}{1+(\delta/\varepsilon)^2} \quad , \qquad (g1)$$

and estimated the parameters M and ε; here $(1+\delta)$ is the frequency divided by the resonant frequency, 2ε is the half-power bandwidth divided by the resonant frequency, so that $(2\varepsilon)^{-1}$ satisfies the usual definition for the "Q-factor" of the resonator, and M is the maximum energy amplification factor at resonance. (The first term of the Taylor series of $K_\alpha(s)$ for s close to a zero s_n also leads to the form (g1)).

Assuming the central resonant frequency to correspond exactly with k = 12, we calculated the values for r_{Sk}^{-2} for a few values of ε and, by interpolation, arrived at $\varepsilon = 0{,}032$ or $Q = 16$ as the best fit of the estimated r_{Sk}^{-2}-values of fig. 10. The maximum energy amplification factor M came out as 570, so that the maximum amplitude amplification factor was estimated to be $(570)^{\frac{1}{2}} \approx 24$.

Fig. 12 gives the estimated real shape of the resonance peak together with the r_{Sk}^{-2}-values from fig. 10.

The rms error in the estimate of Q is believed to be of the order of 10 to 15 percent; that in the estimate of $M^{\frac{1}{2}}$, however, may be well of the order of 20 to 30 percent.

To terminate this section, we just mention that the conspicuous narrowness of the first peaks in the autospectra of Olafsfjördur, at 0,76 mHz (see section e) indicate a "real Q-factor" of the order of 50.

h. Discussion

The estimates for Q and $M^{\frac{1}{2}}$ found in the previous section appear to be relatively high as compared with values found in the literature (13, 11) for rectangular bays with constant depth and similar ratios between entrance width and length: maximum amplitude factors about 5 to 10. The reason of this difference probably is the pronounced funnel-like shape of Eyjafjördur.

It is known that the shape of the resonance peaks in cases like these is determined by two quite different mechanisms provoking dissipation of the wave energy in the basin: 1° turbulent friction caused by the associated oscillating currents and by large eddies; 2° outward energy radiation by waves propagating from the entrance to the open sea. A detailed analysis for Eyjafjördur showed that the first mechanism, in view of the very small oscillating currents in the deep fjord, can only account for a very small part of the total energy dissipation, so that the second mechanism must be the predominant one in this case.

MAIN CONCLUSIONS

1. The existence of the first three modes of natural longitudinal oscillations in the main fjord was demonstrated. The periods are 124, 55 and 35 minutes, respectively.

2. The concept of the fjord responding as a linear passive system on a random input was confirmed to be a good approximation in most cases for periods from 6 hours down to about 30 minutes.

3. In this period range the results could be rather well fitted with the theoretical description for a "model fjord" whose width and depth are given by certain powers of the distance to the closed head of the fjord. For the geometrical parameter α appearing in the theory for such a model fjord, values between -0,05 and +0,3 were found.

4. A detailed analysis of the first resonance peak at 124 minutes resulted in an estimated Q-factor (ratio between resonant frequency and half-power bandwidth) of 16 and an estimated maximum amplification factor of 24.

5. It appeared that the main factor responsible for the dissipation of wave energy in the fjord is the outward radiation of wave energy to the sea.

6. All conclusions above were derived from a number of chart records taken with ordinary float type tide recorders.

ACKNOWLEDGEMENTS

Considerable practical assistance including services by vessel was offered by the Icelandic Department of Ports and Lighthouses. The authors want to express their sincere appreciation to the Office of Naval Research (Grant No 580-17), to the University of Florida's Department of Port and Ocean Engineering, to Professor James Purpura, the University of Florida and to Mr Gunnar Bergsteinsson, Chief Hydrographer, The Icelandic Department of Ports and Lighthouses.

REFERENCES

(1) R.B. Blackman & J.W. Tukey, The Measurement of Power Spectra, 1958 (Dover Publ.).

(2) D.E. Cartwright, M.J. Tucker & D. Catton, Digital techniques for the study of sea waves...., Trans.Soc. Instrum.Technology 14(1), 1962, pp. 1-16.

(3) A. Defant, Physical Oceanography, Vol. 11, 1961 (Pergamon). See Chapter VI.

(4) R. Dorrestein, Amplification of long waves in bays, Engineering Progress at the University of Florida, XV(12), Tech.Paper No. 213, 1961.

(5) J.J. Dronkers, Tidal Computations in Rivers and Coastal Waters, 1964 (North-Holland Publishing Company). See Chapter VIII.

(6) J.N. Hunt, Tidal oscillations in estuaries, Geophys J. Royal Astron.Soc. 8(4), 1964, pp. 440-455.

(7) Li-San Hwang & E.O. Tuck, On the oscillations of harbours of arbitrary shape, J.Fluid Mech. 42(3), 1970, pp. 447-64.

(8) E. Jahnke & F. Emde, Tables of functions, 4th edition, 1945 (Dover Publ.). See p. 146 middle and p. 127.

(9) H. Lamb, Hydrodynamics, 6th edition 1932 (1945) (Dover Publ.). See art. 185, 186.

(10) Jiin-Jen Lee, Wave induced oscillations in harbours of arbitrary geometry, J.Fluid Mech. 45(2), 1971, pp. 375-94.

(11) T. Momoi, A Long Wave in a Rectangular Bay - Case of Normal Incidence, Bull. Earthquake Res.Inst.Univ. of Tokyo 48(5), 1970, pp. 871-91 and earlier publications of this author in the same journal.

(12) W.H. Munk & D.E. Cartwright, Tidal Spectroscopy and Prediction, Phil.Trans.Roy.Soc. London Series A No. 1105, Vol. 259, 1966, pp. 533-581. See appendix B, p. 580.

(13) F. Raichlen, Harbor Resonance, Chapter 7 in "Estuary and Coastline Hydrodynamics" (A.T. Ippen, editor) 1966 (McGraw-Hill).

(14) J.C. Schönfeld, Tides in funnel-shaped channels, Rijkswaterstaat Nota CSD 55-16 N, (The Hague), 1955.

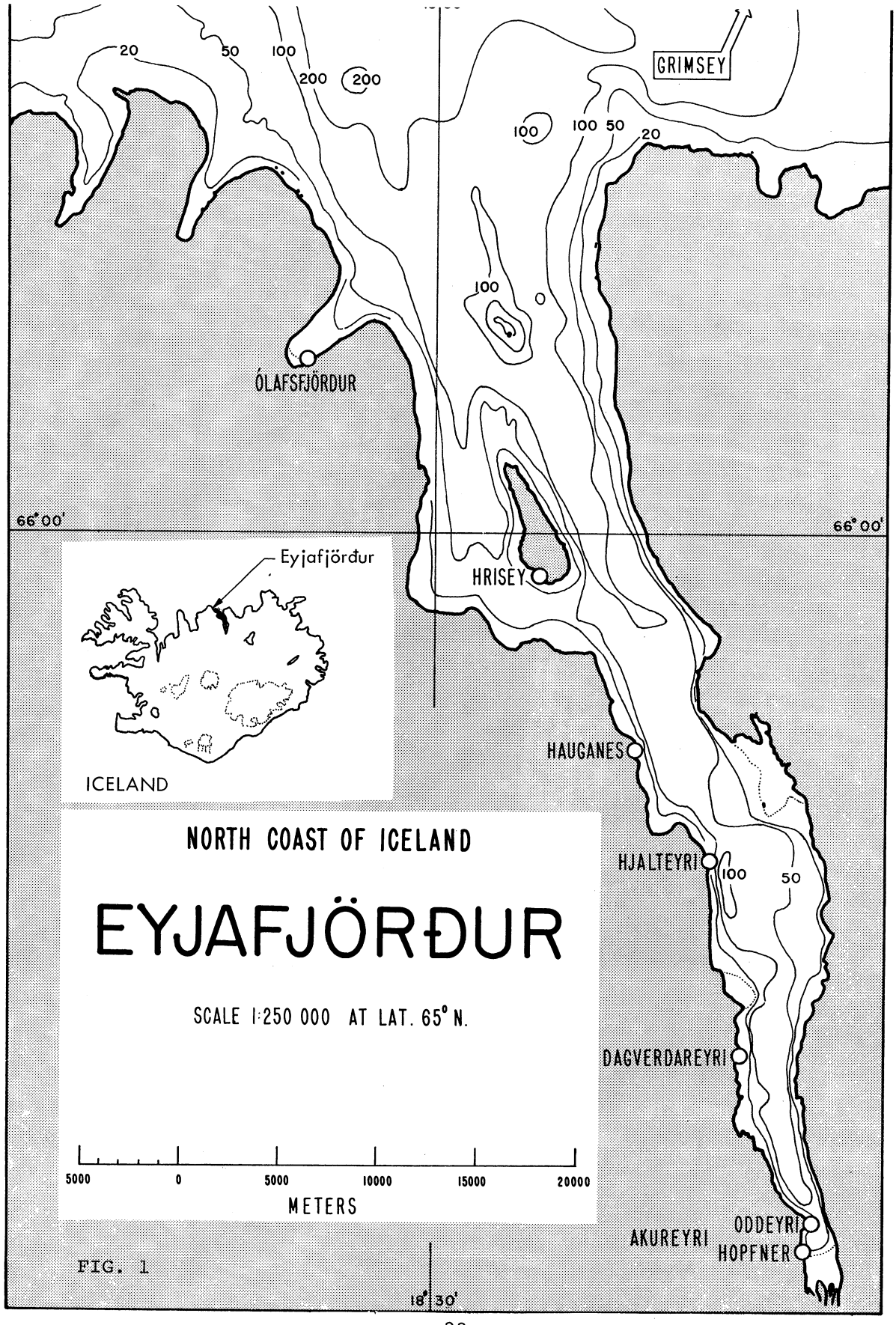
20
50
100
200
200
100
100
50
20
GRIMSEY
100
0
ÓLAFSFJÖRDUR
66° 00'
66° 00'
Eyjafjörður
HRISEY
ICELAND
HAUGANES
HJALTEYRI
100
50
NORTH COAST OF ICELAND
EYJAFJÖRÐUR
SCALE 1:250 000 AT LAT. 65° N.
DAGVERDAREYRI
5000
0
5000
10000
15000
20000
METERS
AKUREYRI
ODDEYRI
HOPFNER
18° 30'

FIG. 1

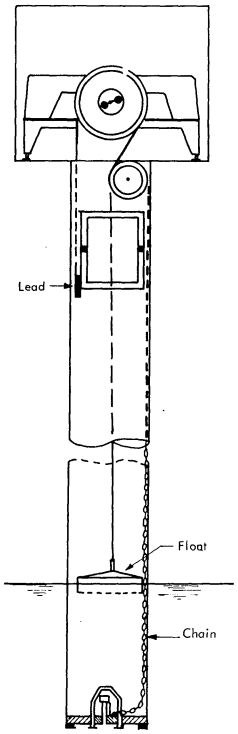

FIG. 2

Captions to figures

Fig. 3 Plot of width b and mean depth d against distance x. Linear - linear.

Fig. 4 The same but double logarithmic.

Fig. 5 Two autospectra. Segments nr. 5 and 6.

Figs. 6-9 Plots of amplitude ratio r and phase difference ϕ between a station and Akureyri S.

Meaning of symbols

smallest W_k or $\bar{W}$ value	symbols
> 10 x 80 mm^2/mHz	⊕ ————
1 to 10 x " " "	+ ————
0,1 to 1 x " " "	x — — —
0,01 to 0,1 x " " "	< --------

Fig. 10 Crosses: estimated values for amplitude ratio r_{Sk} between the sea off the entrance and Akureyri, and for r_{Sk}^{-1}. Circles: pre-assumed values for r_{Sk} and r_{Sk}^{-1} (see text). Dotted line: estimated "real" amplitude ratio (ref. fig. 12).

Fig. 11 Spectral window function P(|k-f|).

Fig. 12 Crosses: estimated values for r_{Sk}^{-2} = square of amplitude ratio between Akureyri and the sea off the entrance. Circles: ref. fig. 10.

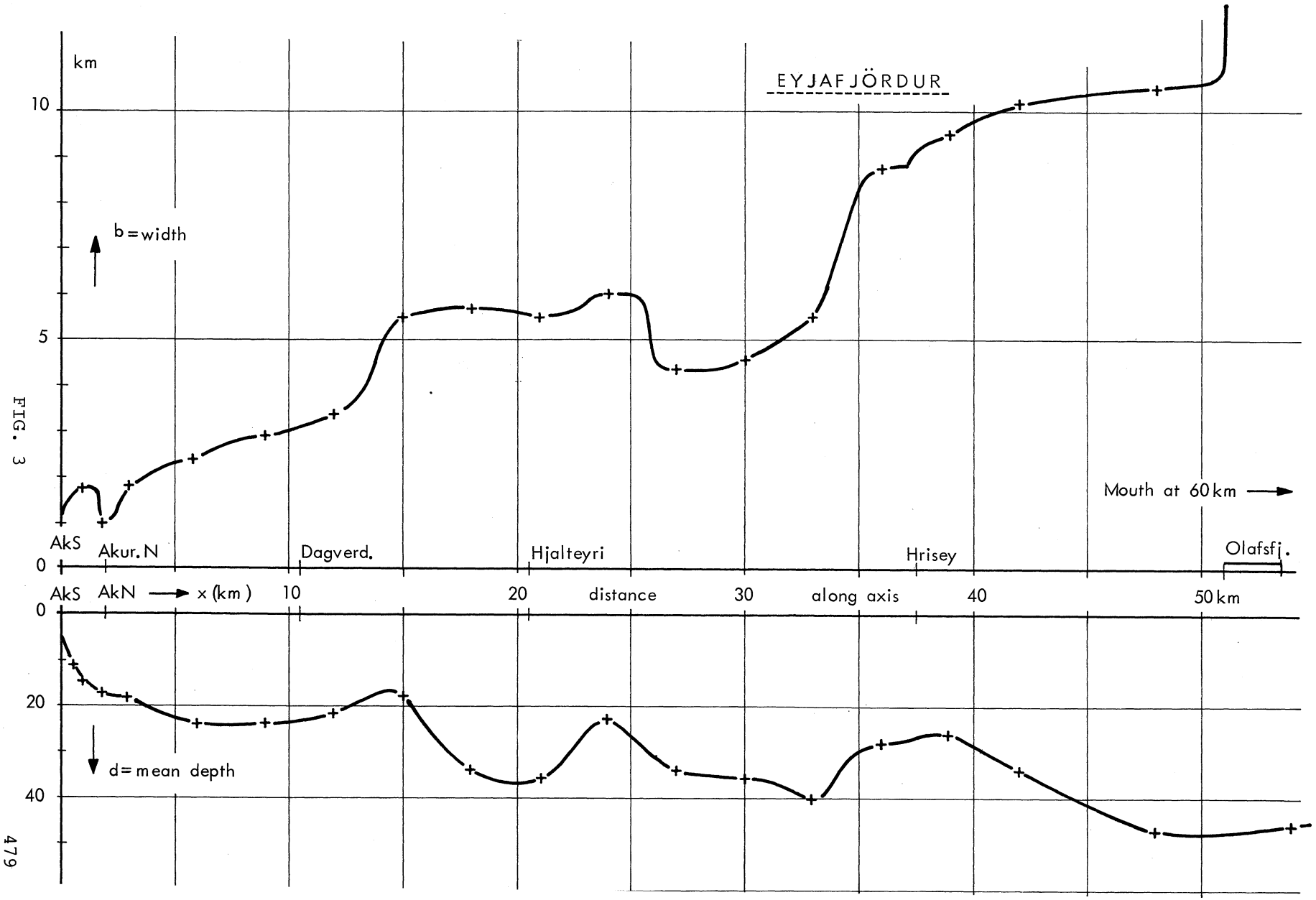
km
EYJAFJÖRDUR
10
5
0
b = width
Mouth at 60 km
AkS
Akur. N
Dagverd.
Hjalteyri
Hrisey
Olafsfj.
AkS
AkN
x (km)
10
20
distance
30
along axis
40
50 km
0
20
40
d = mean depth

FIG. 3

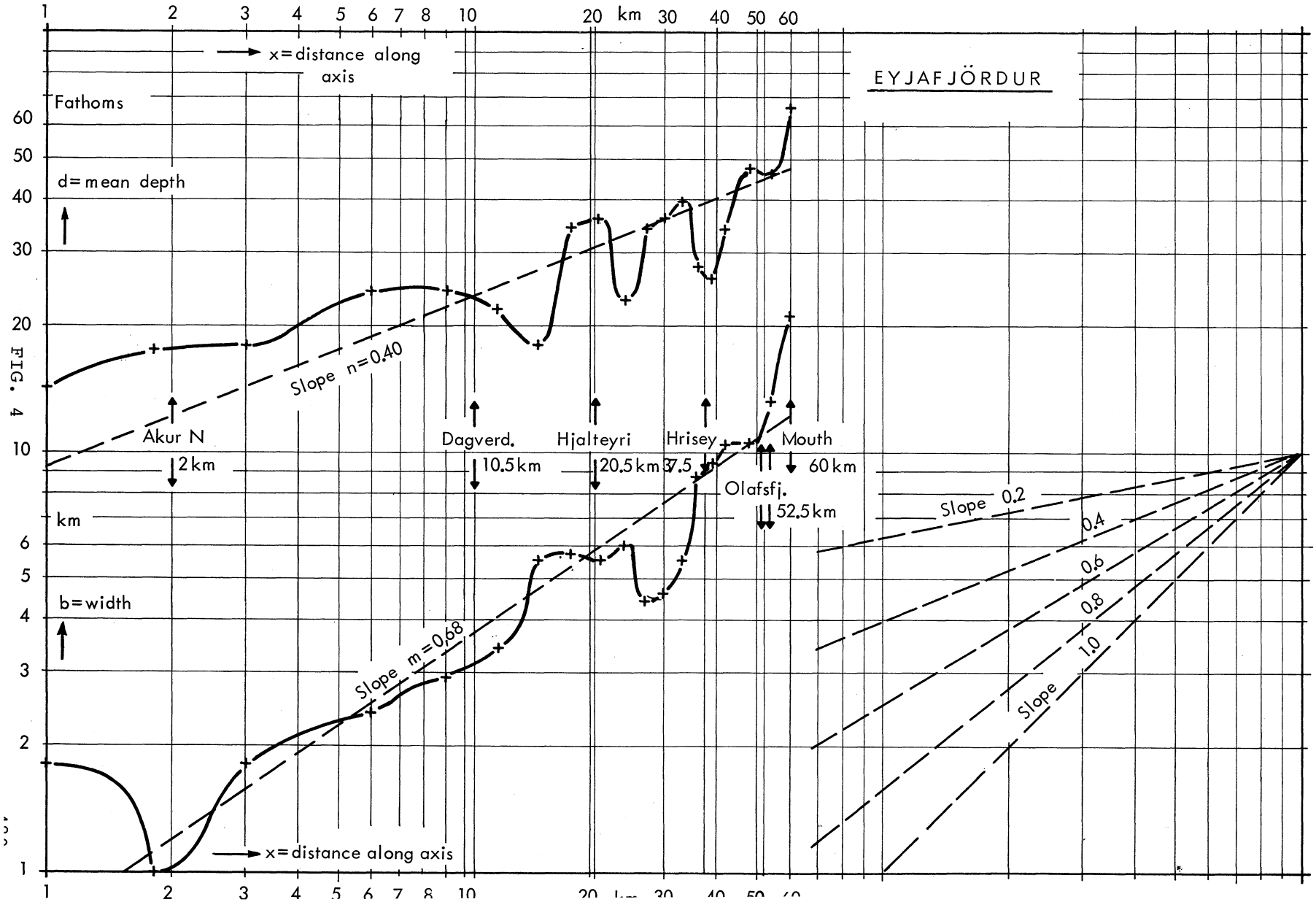
EYJAFJÖRDUR
x=distance along axis
Fathoms
d=mean depth
Slope n=0.40
Akur N
2km
Dagverd.
10.5km
Hjalteyri
20.5km
Hrisey
37.5
Olafsfj.
52.5km
Mouth
60km
km
b=width
Slope m=0.68
Slope 0.2
0.4
0.6
0.8
1.0
Slope
x=distance along axis

FIG. 4

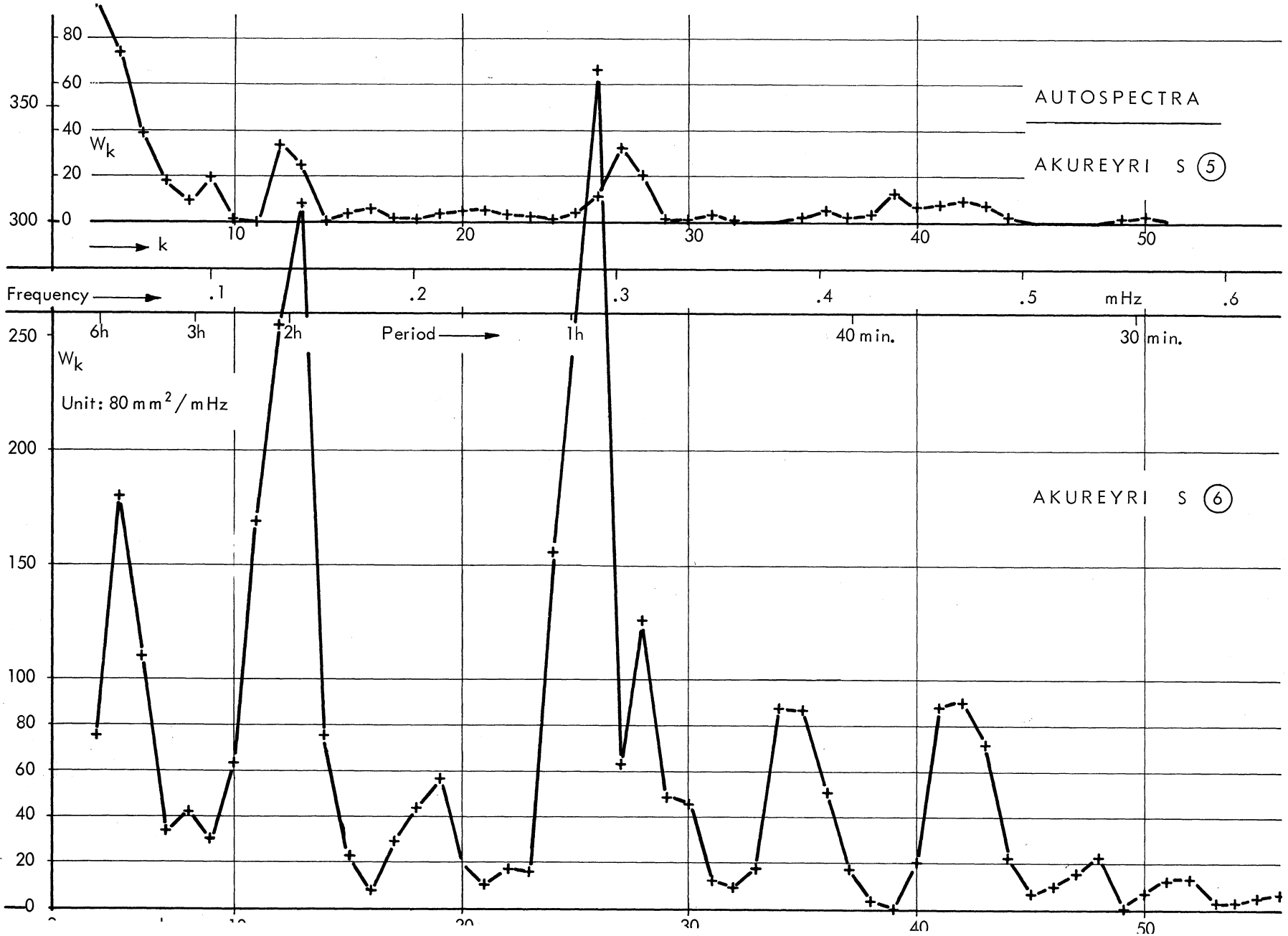
AUTOSPECTRA
AKUREYRI S (5)
AKUREYRI S (6)
W_k
k
Frequency
mHz
Period
6h
3h
2h
1h
40 min.
30 min.
Unit: 80 mm²/mHz

FIG. 5

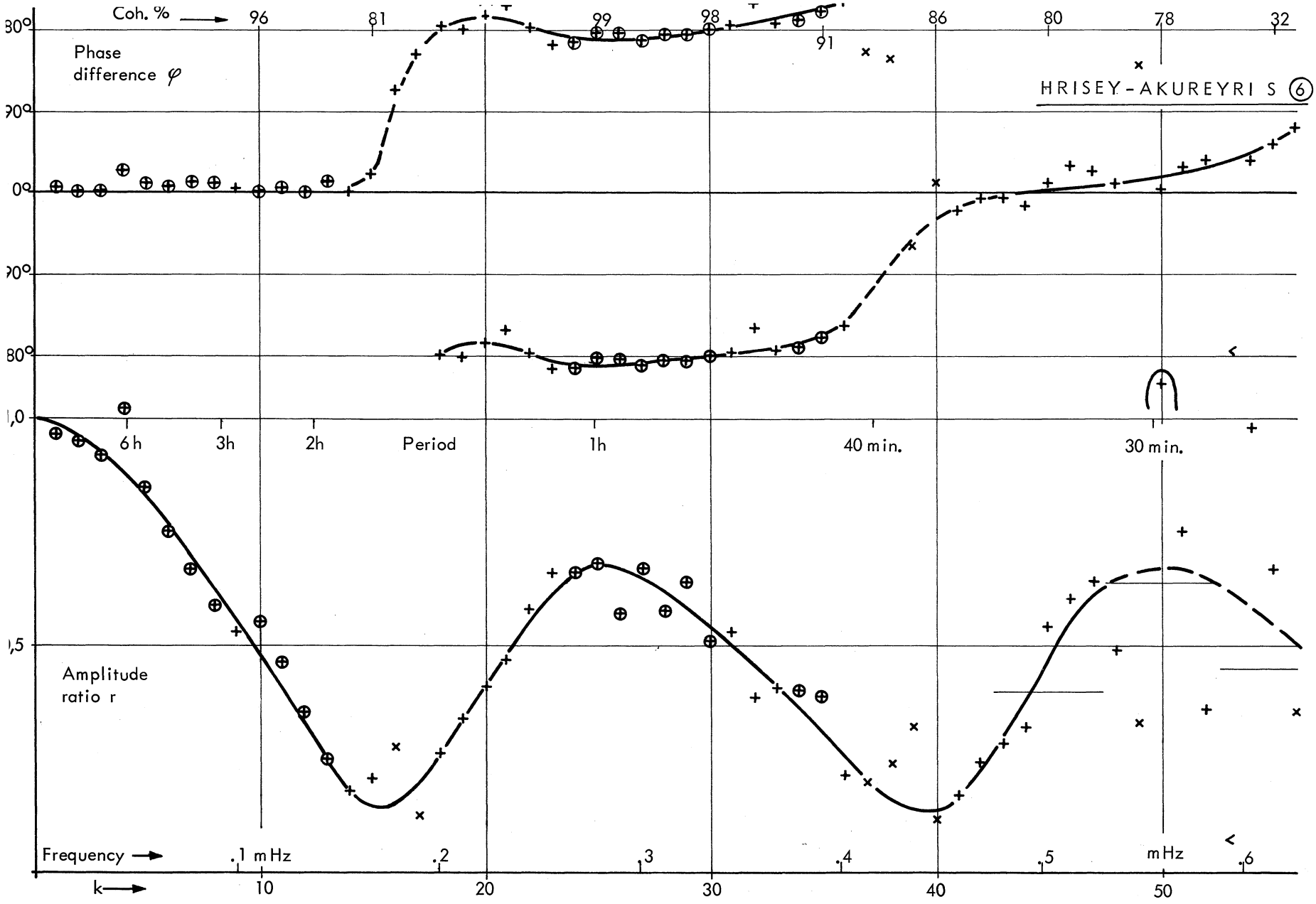
Coh. %
96
81
99
98
91
86
80
78
32
Phase
difference φ
HRISEY - AKUREYRI S ⑥
6 h
3h
2h
Period
1h
40 min.
30 min.
Amplitude
ratio r
Frequency
.1 mHz
.2
.3
.4
.5
mHz
.6
k
10
20
30
40
50

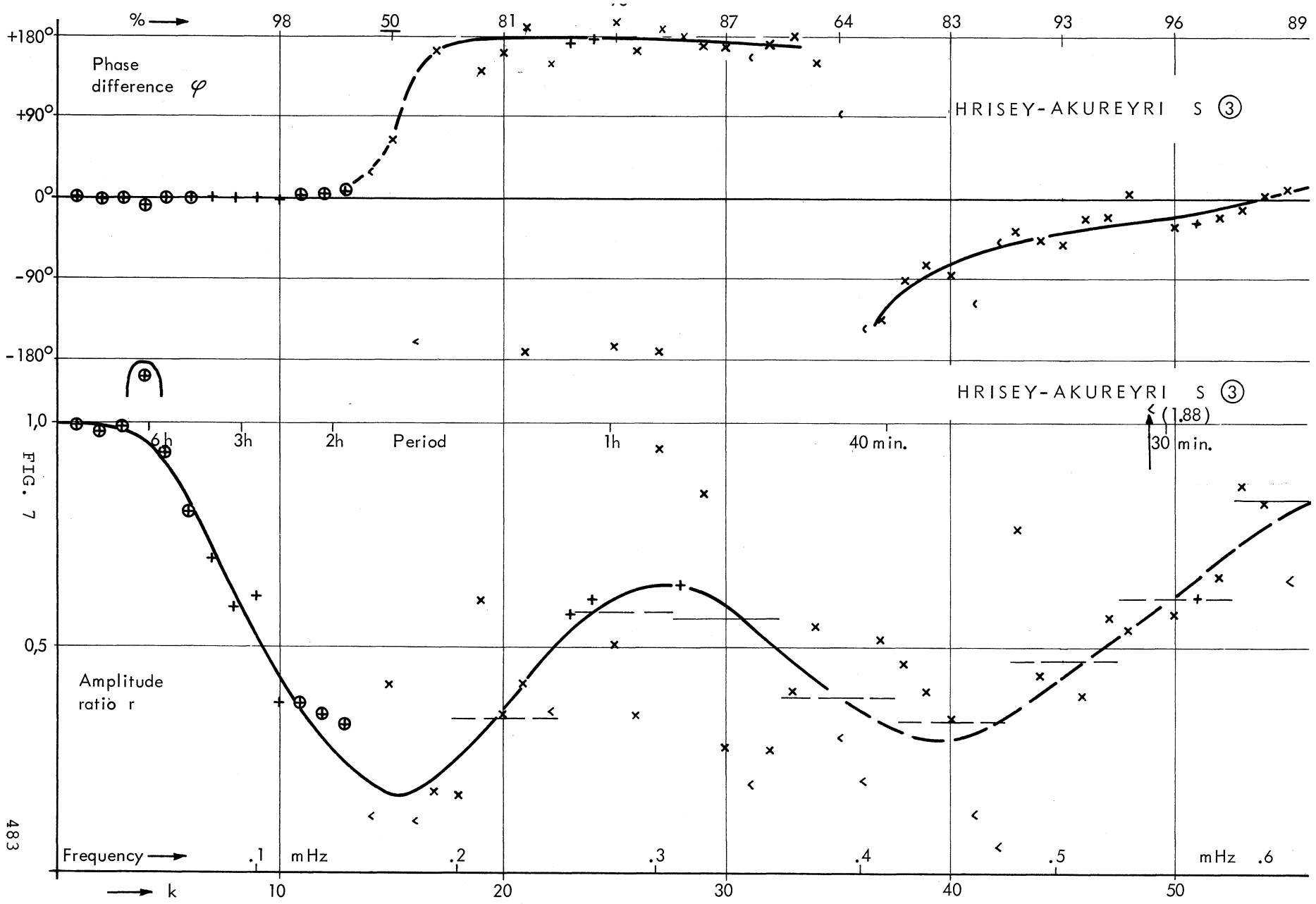
%
98
50
81
87
64
83
93
96
89
+180°
+90°
0°
-90°
-180°
Phase
difference φ
HRISEY-AKUREYRI S ③
HRISEY-AKUREYRI S ③
1,0
0,5
6h
3h
2h
Period
1h
40 min.
30 min.
(1.88)
Amplitude
ratio r
Frequency
.1
mHz
.2
.3
.4
.5
mHz
.6
k
10
20
30
40
50

FIG. 7

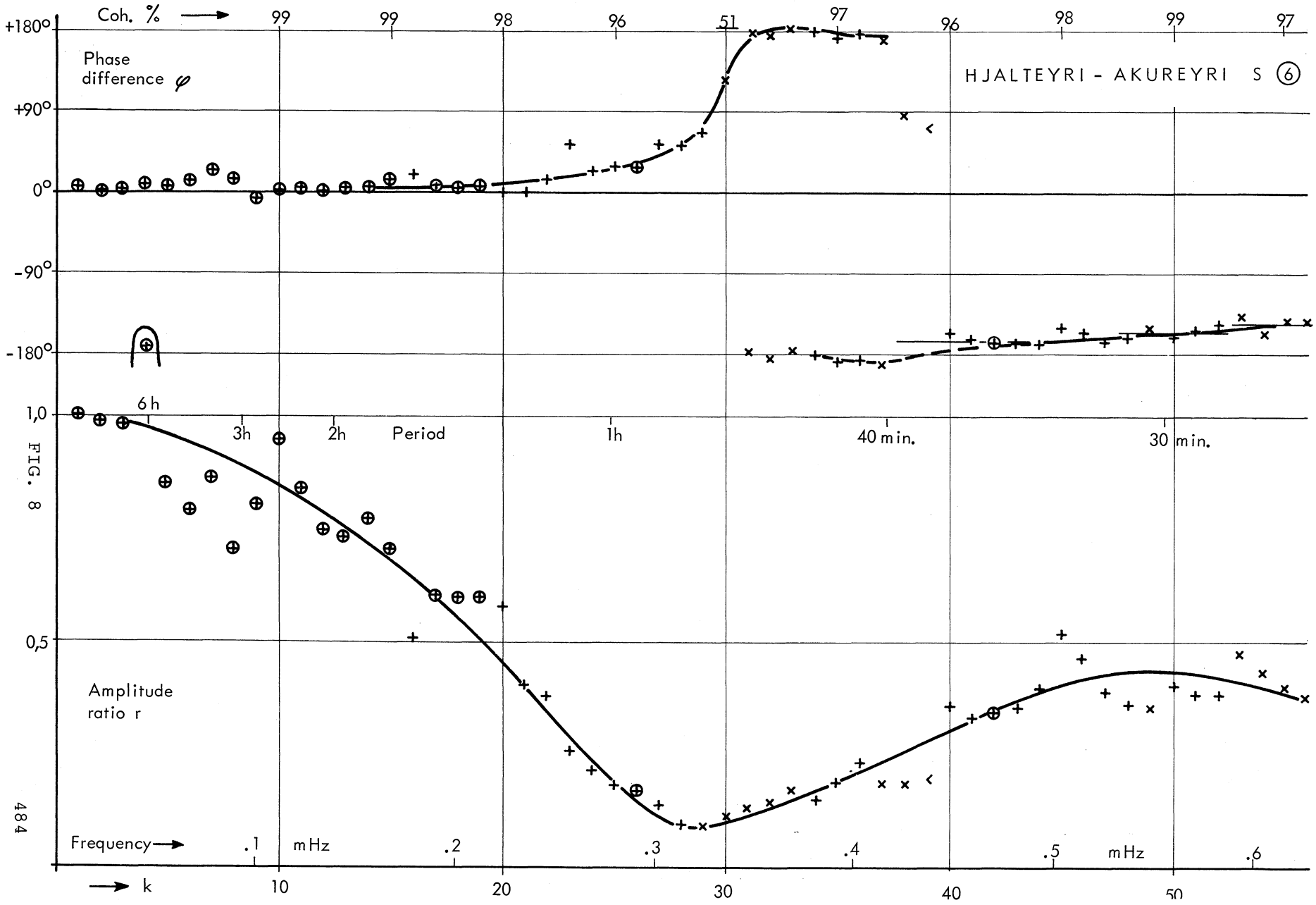
Coh. % →
99
99
98
96
51
97
96
98
99
97
+180°
+90°
0°
-90°
-180°
Phase
difference φ
HJALTEYRI - AKUREYRI S ⑥
6 h
3h
2h
Period
1h
40 min.
30 min.
1,0
0,5
Amplitude
ratio r
Frequency →
.1
mHz
.2
.3
.4
.5
mHz
.6
→ k
10
20
30
40
50

FIG. 8

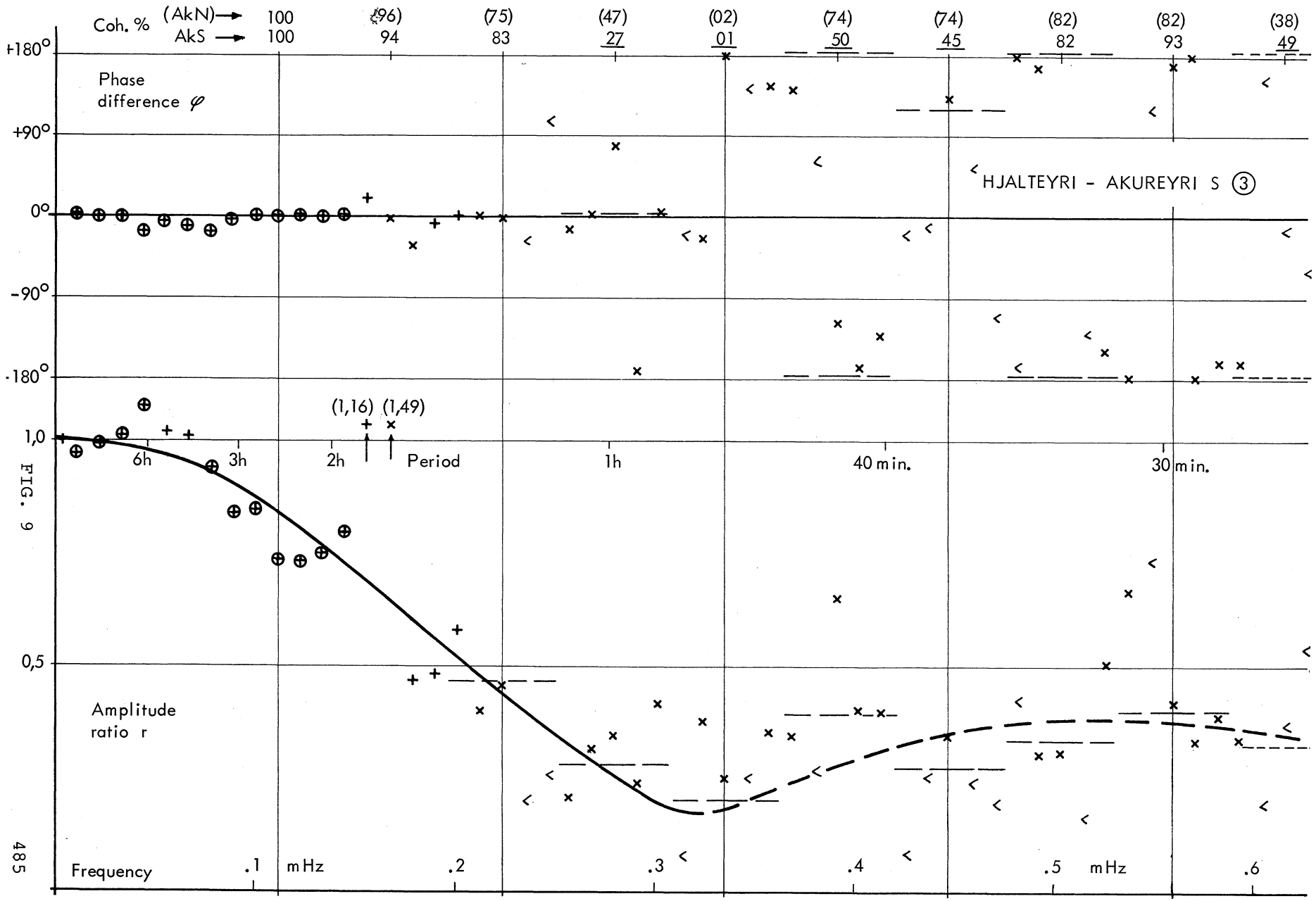
Coh. %
(AkN)→ 100 (96) (75) (47) (02) (74) (74) (82) (82) (38)
AkS → 100 94 83 27 01 50 45 82 93 49
+180°
Phase
difference φ
+90°
0°
-90°
-180°
HJALTEYRI - AKUREYRI S ③
(1,16) (1,49)
1,0
6h
3h
2h
Period
1h
40 min.
30 min.
FIG. 9
0,5
Amplitude
ratio r
Frequency
.1
mHz
.2
.3
.4
.5
mHz
.6

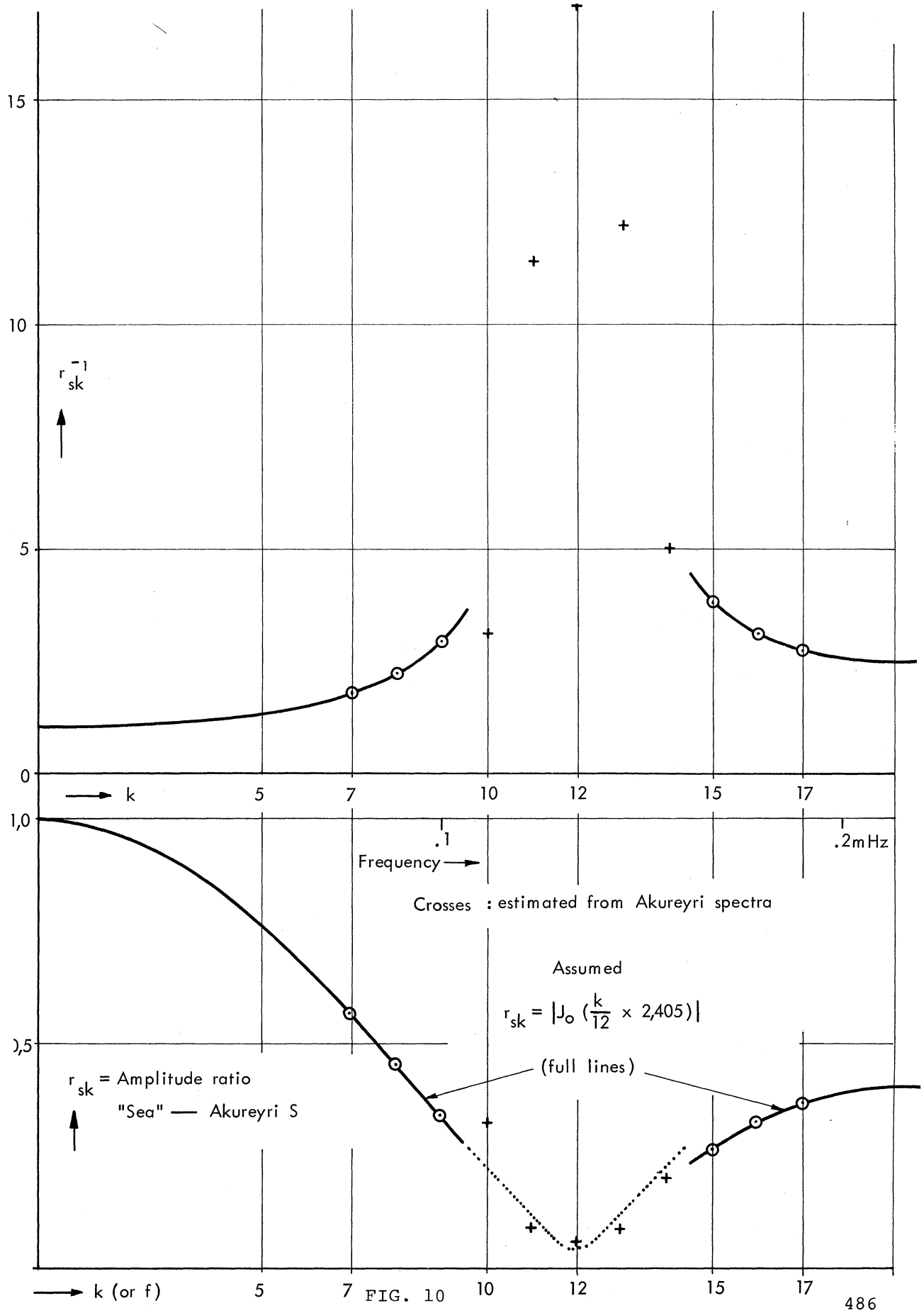
15
10
5
0
r_{sk}^{-1}
k
5
7
10
12
15
17
1,0
0,5
.1
Frequency
.2mHz
Crosses : estimated from Akureyri spectra
Assumed
$r_{sk} = |J_o(\frac{k}{12} \times 2{,}405)|$
(full lines)
r_{sk} = Amplitude ratio
"Sea" — Akureyri S
k (or f)

FIG. 10

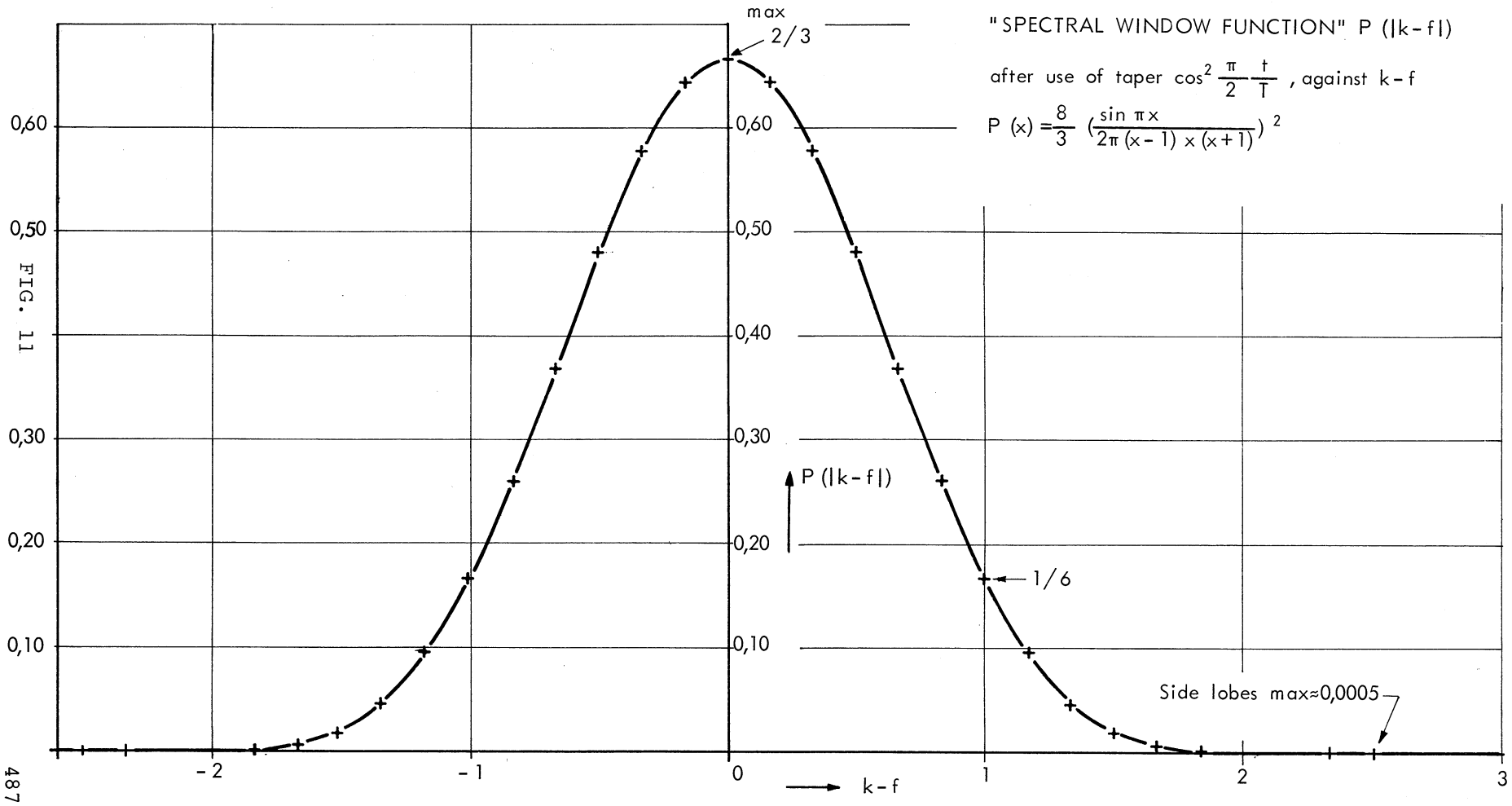
"SPECTRAL WINDOW FUNCTION" P (|k-f|)
after use of taper $\cos^2 \frac{\pi}{2} \frac{t}{T}$, against k-f
$P(x) = \frac{8}{3} \left(\frac{\sin \pi x}{2\pi (x-1) \times (x+1)}\right)^2$
max
2/3
1/6
Side lobes max≈0,0005
P (|k-f|)
k-f
0,60
0,50
0,40
0,30
0,20
0,10
-2
-1
0
1
2
3

FIG. 11

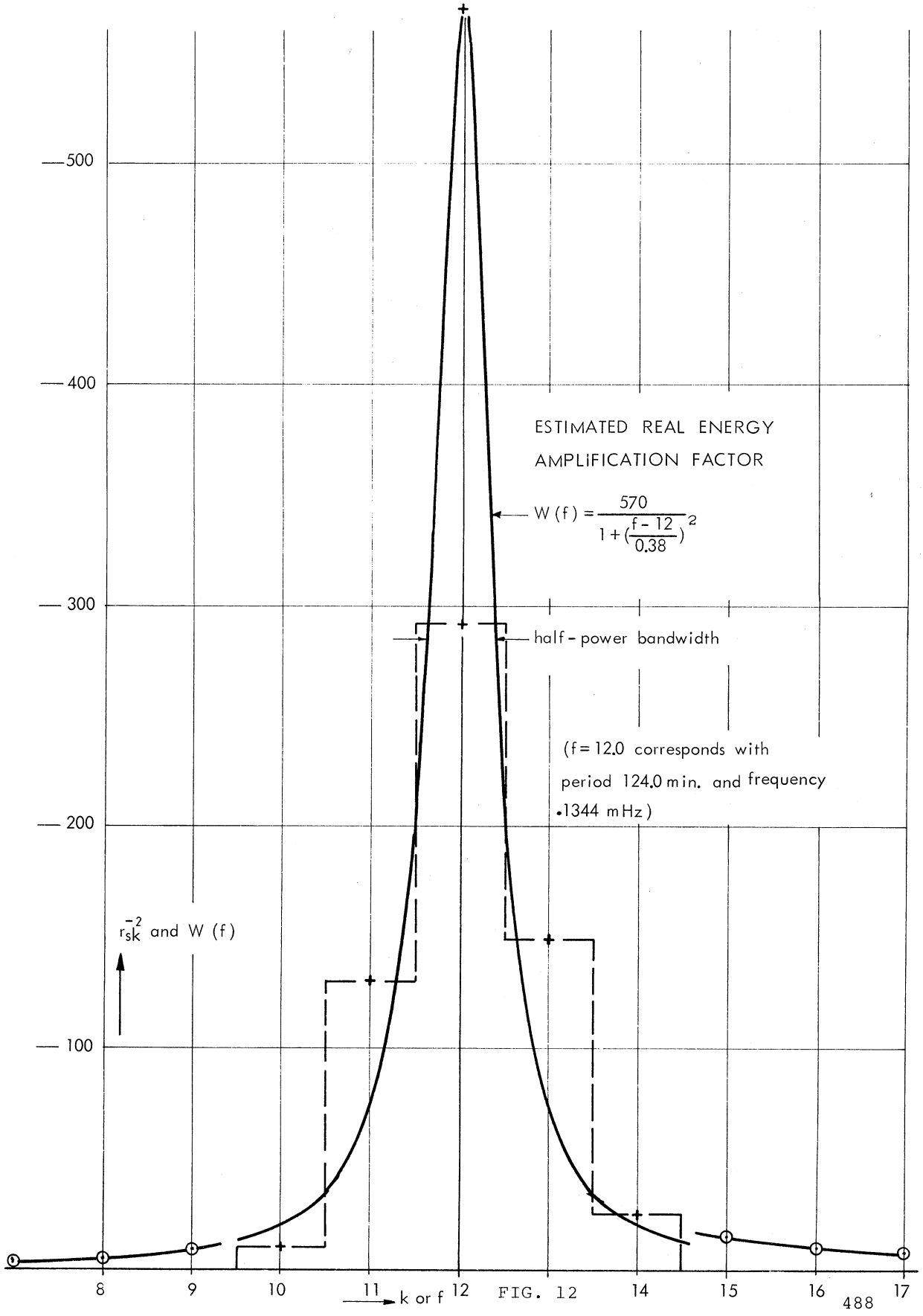
500
400
300
200
100
ESTIMATED REAL ENERGY
AMPLIFICATION FACTOR
$W(f) = \frac{570}{1+(\frac{f-12}{0.38})^2}$
half-power bandwidth
(f = 12.0 corresponds with
period 124.0 min. and frequency
.1344 mHz)
r_{sk}^{-2} and W (f)
8
9
10
11
k or f
12
14
15
16
17

FIG. 12